

Hierarchical Intention-Aware Expressive Motion Generation for Humanoid Robots

Lingfan Bao, Yan Pan, Tianhu Peng, Kanoulas Dimitrios and Chengxu Zhou

Abstract—Effective human-robot interaction requires robots to identify human intentions and generate expressive, socially appropriate motions in real-time. Existing approaches often rely on fixed motion libraries or computationally expensive generative models. We propose a hierarchical framework that combines intention-aware reasoning via in-context learning (ICL) with real-time motion generation using diffusion models. Our system introduces structured prompting with confidence scoring, fallback behaviors, and social context awareness to enable intention refinement and adaptive response. Leveraging large-scale motion datasets and efficient latent-space denoising, the framework generates diverse, physically plausible gestures suitable for dynamic humanoid interactions. Experimental validation on a physical platform demonstrates the robustness and social alignment of our method in realistic scenarios.

I. INTRODUCTION

In human society, communication takes place through two primary channels: verbal and non-verbal. While verbal language conveys explicit information, non-verbal cues, such as facial expressions, body posture, and gestures, carry rich and socially signals that reflect intention, emotion, and context. These expressive cues play a crucial role in natural interaction and mutual understanding for human robot interaction [1]. Among various robotic embodiments, humanoid robots are uniquely suited to support non-verbal social communication [2]. Their anthropomorphic structure allows for human-like motion and gesture execution, making them ideal for conveying expressive intent and enhancing user engagement in human-robot interaction [3], [4].

On one hand, current research in humanoid robotics has made significant progress in motion control, focusing primarily on locomotion [5], [6], and manipulation [7]. These approaches aim for physical robustness and task execution, but often overlook the role of expressive, socially meaningful motions. On the other hand, human-robot interaction (HRI) research emphasises communication and social engagement, frequently using language-based interfaces [4], [8] or rule-based behavioural templates [9], [10]. However, these systems often lack physical embodiment, and rarely adaptively express nuanced human-like gestures in response to dynamic interaction contexts. Despite progress in both domains, there remains a fundamental disconnect: few systems are capable

of interpreting human intention and generating appropriate upper-body expressive gestures in real time. This limits the ability of humanoid robots to participate in socially natural, co-present interaction scenarios.

To develop a flexible and scalable framework that allows humanoid robots to perceive social cues and autonomously generate natural in real-time interactions, we introduce a scalable, intention-aware framework HIAER for expressive humanoid responses that integrates a large vision-language model (VLM) with real time generative motion control, enabling social interactions grounded in perception, intent inference, and gesture execution. We firstly leverage the in-context learning [11], [12] capability of VLMs to interpret human intention based on prompt and body language. The model generates structured gestural prompts that reflect the inferred social context. At the motion planning lay, we utilize a text-to-motion diffusion model [13] to produce temporally coherent and socially expressive motion sequences in real time, conditioned on the high-level prompts. Finally, the motion will be conducted through a low-level controller to execute the generated motion on a physical humanoid platform.

Our system empowers humanoid robots to produce socially aligned, physically executable gestures in real time. The key contributions of this work are in conclusion:

- We present a low-latency, end-to-end framework that is validated through physical execution on a humanoid platform, demonstrating its effectiveness in real-world human-robot interaction tasks.
- We introduce an iterative intention refinement, allowing the robot to adjust its response based on real-time feedback from human behaviour and history information.
- We introduce a fallback strategy that generates cautious and socially appropriate gestures under ambiguous or low-confidence predictions.

In our experiments, we evaluate the proposed framework across five representative categories of real-world human-robot interactions. The system achieves execution success in real robot, and demonstrates strong intention refinement capabilities, robust fallback behavior under ambiguous inputs, and context-sensitive gesture selection grounded in social cues.

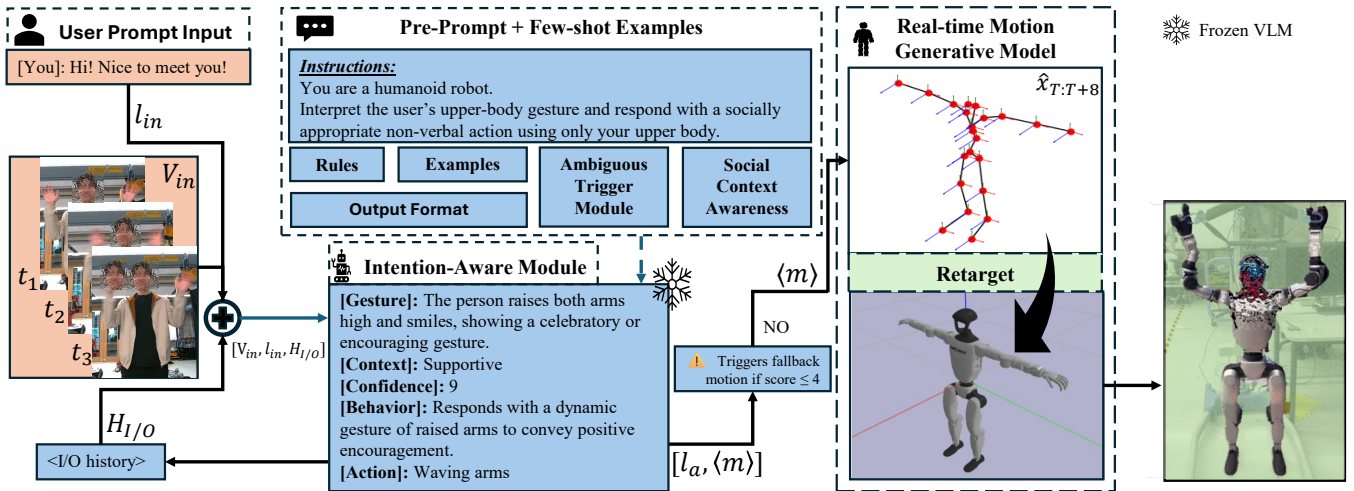


Fig. 1: Overall framework of the proposed work. The system receives multi-modal user inputs, vision, language, and I/O history, and fuses them for gesture interpretation. A frozen VLM, guided by a pre-defined prompt and few-shot examples, infers the user’s intent and selects a context-appropriate gesture. If confidence is low, a fallback policy is triggered. The selected action is sent to a real-time motion generation module DART and retargeted for execution on a physical robot. Pink represents input modalities; Blue represents intention-aware reasoning; Green represents motion synthesis and execution. Dashed arrows denote initial one-time inputs, and solid arrows indicate inputs continuously provided throughout interaction.

II. RELATED WORK

A. Expressive Human-Robot Interactions

Non-verbal communication plays a critical role in human interactions, conveying emotions, intentions, and social cues beyond spoken language. Recent studies have shown that when interacting with AI agents, users expect not only coherent verbal responses but also appropriate gestures and postures that align with the conversational context [4]. In addition, previous works have demonstrated that enabling robots to generate expressive motions significantly enhances communication quality and user engagement during human-robot interaction [14].

While recent frameworks have enabled humanoid robots to execute diverse and expressive motions, they often lack the ability to engage in intention-aware interactions with humans. For example, ExBody [15] enables humanoid robots to learn upper-body expressive motions through imitation learning from large-scale human motion datasets and generative models. Similarly, OmniH2O [16] demonstrates a system capable of producing a wide range of whole-body motions using data-driven techniques. However, these works primarily focus on motion execution itself, without considering how to select or adapt motions in response to dynamic human social cues.

Traditional methods for expressive human-robot interaction behaviors generally fall into two categories: rule-based and template-based. Rule-based methods rely on predefined rules, offering predictability but limited adaptability to dynamic social contexts [9], [10], [17]. Template-based methods use motion templates from expert demonstrations to increase flexibility but still impose rigid structural constraints, limiting diverse and context-sensitive behavior generation.

The rapid advancement of large language models and VLMs has significantly enhanced robots’ ability to understand and reason about human intentions across diverse and dynamic scenarios. In the field of legged robotics, recent works have primarily leveraged LLMs and VLMs to solve task-oriented problems such as locomotion planning and control [18], [19]. In contrast, our work employs ICL with few-shot examples to teach the agent to reason about human intentions and respond through corresponding expressive gestures. Rather than focusing solely on task execution, we utilize LLMs to infer human social cues and generate appropriate upper-body actions for humanoid robots in real-time interactions.

B. Expressive Motion Generation

Generating expressive and natural motions is critical for effective human-robot interaction, as it enables robots to clearly convey social intent and respond dynamically in real-world contexts. Current data-driven approaches broadly include retrieval-based methods and generative models. Retrieval methods select motion sequences from existing databases, offering realism and quick inference but limited flexibility due to library constraints.

Generative models, such as GANs [20], VAEs [21], and diffusion models [22], allow for novel and contextually adaptable motions but often require intensive training and computational resources. Diffusion-based models, in particular, have demonstrated exceptional capabilities in generating diverse, high-quality motions, such as MDM [23]. Recent models like DART [13] further support real-time performance through efficient latent-space denoising conditioned on textual descriptions and spatial constraints.

Large-scale motion datasets, such as AMASS [24], HumanML3D [25] facilitate training compact yet powerful

generative models, effectively bridging the gap between high-level human intent and low-level motion execution. However, existing frameworks like EMOTION++ [12] and GenEM [26] still rely significantly on demonstration-based methods or predefined templates, limiting their adaptability and naturalness.

Our proposed approach integrates real-time human intention inference, leveraging ICL, with a diffusion-based generative model DART [13]. By capitalizing on structured datasets and a streamlined text-to-motion interface, our framework produces diverse, socially appropriate, and physically executable motions, enhancing real-time humanoid robot interactions.

III. HIERARCHICAL INTENTION-AWARE EXPRESSIVE FRAMEWORK

A. Overview

As illustrated in Fig. 1, HIAER (Hierarchical Intention-Aware Expressive Action for Humanoid Robot) is designed as a hierarchical framework composed of three functional modules, each responsible for a distinct stage of processing: (i) Vision capture module, (ii) Intention-aware module, and (iii) Real-time motion generation and execution Module.

The system takes as input a user image observation O_{in} and a natural language prompt l_{in} . These inputs are first processed by the *Intention-Aware Module*, which serves as the strategy-level component of the framework. This module outputs a structured motion prompt, decomposed into a sequence of short expressive motion clips m_i , each representing a temporally coherent gesture segment. Additionally, both input and output information are logged into a rolling interaction history buffer denoted as $H_{I/O}$, which supports iterative refinement and context-aware reasoning across time.

These motion clips are passed into the real-time generation model DART, which synthesizes human skeleton motion sequences as reference trajectories. These reference motions are then retargeted to the G1 humanoid robot model. To ensure smooth and responsive execution, we perform high-frequency interpolation on the 25 FPS motion output, upsampling it to 500 Hz. The resulting joint trajectories are temporally aligned and converted into continuous position references. The DART module operates online, continuously generating a short motion horizon $\hat{x}_{T:T+8}$, which is fed into a low-level PD tracking controller to compute real-time torque commands τ_t .

B. Intention-Aware Strategy Planning

We implement intention reasoning via ICL with GPT-4o [27], a VLM that fuses visual and linguistic cues. The inputs, including the robot’s visual observation V_{in} and/or the optional user’s language instruction l_{in} , provide essential social context that the robot must interpret and respond to appropriately. To enhance temporal coherence and contextual understanding, we maintain an interaction history buffer $H_{I/O}$, which stores past user

inputs and corresponding robot outputs. These signals are collectively passed into a Vision-Language agent $f(V_{\text{in}}, l_{\text{in}}, H_{I/O})$, which is guided by chain-of-thought prompting to generate a high-level social context analysis l_a and a structured motion primitive $\langle m \rangle$. Formally, we define

$$[l_a, \langle m \rangle] = f(V_{\text{in}}, l_{\text{in}}, H_{I/O}). \quad (1)$$

To infer expressive motion strategies from high-level human input, We structure the instructional prompt to the VLM with two components: a pre-defined system prompt that defines the robot’s role, several few-shot examples consisting of human intent and corresponding robot gesture responses.

The pre-prompt first defines the VLM’s role as a non-verbal social agent—tasked with inferring human intent and selecting the corresponding upper-body gesture. Then, the VLM is instructed to output responses in a structured format comprising five fields: We enforce a structured output containing five fields: (i) Description, a concise summary of the observed person pose; (ii) Interaction Context, classification of the pose into one of the predefined social intent categories; (iii) Confidence Score, an integer between 1 to 10 reflecting confidence in the inferred interaction context; (iv) Robot Behavior, a brief nonverbal response description; and (v) Motion, the chosen primitive gesture to execute.

Additionally, the Confidence Score encodes the model’s certainty in its context classification; if the score is ≤ 4 , a safe fallback gesture (e.g., *cross arms*) is automatically selected to maintain robust behavior under uncertainty. Social-context awareness is achieved via a rolling history buffer $H_{I/O}$ of past user–robot exchanges, enabling the model to adapt its reasoning to individual familiarity and evolving interaction dynamics.

Together, this constrained output format—combined with confidence-aware fallbacks and social-history conditioning—ensures that VLM responses are both machine-parseable and aligned with safety and social-norm requirements for real-time human–robot interaction.

C. Text-to-Motion Generation Module

The text-to-motion module serves as a flexible interface between high-level intention planning and low-level motor execution, enabling a modular and scalable system design. We adopt DART [13], a diffusion-based motion generation model that produces natural and temporally coherent human motion sequences conditioned on textual prompts.

To ensure smooth transitions and executable outputs, the instruction from the strategy-level module is constrained to short, structured prompts (e.g., “wave hands”). The model generates motion reference clips in an online manner based on predicted future windows.

Each motion segment is represented by a fixed-length trajectory with dimensionality $D = 276 \times N$, where N is the number of frames in the future prediction window.

The output includes the body root translation \mathbf{t} , root orientation R , local joint rotations θ , and joint positions \mathbf{J} , all defined in the SMPL coordinate space.

D. Motion Representation and Retargeting

To facilitate real-time human-to-robot motion transfer, we bridge the morphological gap between human pose data and robot execution on the Unitree G1 humanoid platform [28], which stands 130 cm tall and features 29 actuated upper-body joints. We adopt a diffusion-based generative model that outputs human motion sequences compatible with the SMPL representation, comprising a global root translation $\mathbf{t} \in \mathbb{R}^3$ and joint rotations encoded in a continuous $6D$ rotation format [29].

For effective retargeting to the G1 robot, we employ a lightweight neural network trained to map SMPL pose data directly to robot joint configurations. We construct paired training samples (x_i, y_i) , where $x_i = q_{\text{SMPL},i} \in \mathbb{R}^{135}$ (comprising 22×6 joint rotations plus a $3D$ root translation) and $y_i = q_{\text{robot},i} \in \mathbb{R}^{29}$ are corresponding robot joint angles. This neural mapping is optimized with a Mean Squared Error loss:

$$\text{LMSE} = \frac{1}{N} \sum_i \|f_\theta(x_i) - y_i\|^2, \quad (2)$$

where f_θ denotes the retargeting network parameters and N represents the number of training samples. This method ensures low-latency retargeting, supporting smooth, real-time motion execution on the robot.

IV. EXPERIMENTS

A. Experimental Setup

We conducted our experiments using the Unitree G1 humanoid robot. Additionally, an Intel RealSense D405 camera is integrated to provide high-resolution RGB-D input for upper-body gesture understanding. The intention inference and motion generation modules are powered by large-scale language and vision-language models. All models were executed on a workstation equipped with an Intel Core i9–14900K CPU and an NVIDIA GeForce RTX 4090 GPU.

B. Demonstration Scenarios

To evaluate the system’s capacity for intention understanding and gesture generation, we define a set of representative HRI scenarios, illustrated in Fig. 2. Each case involves a human performing a socially meaningful upper-body motion, and the robot responding based on inferred intent, context, and confidence. We categorize these scenarios into six distinct interaction types:

a) Greeting: The user initiates contact through gestures such as waving or extending a hand for a handshake (Fig. 2(a)–(b)). These cues reflect friendliness or a desire to engage, and the robot responds with socially appropriate gestures, such as waving back or mimicking a handshake.

b) Neutral: When the user stands in a passive posture with no explicit gesture (Fig. 2(c)), the robot maintains a neutral stance to reflect the lack of strong social intent. This serves as a baseline for non-initiated interaction.

c) Supportive Feedback: In celebratory or affirming contexts, the user may raise both arms or perform upbeat gestures (Fig. 2(e)). The robot mirrors this intent with enthusiastic motions, such as waving both arms, to reflect emotional alignment.

d) Defensive Interpretation: Gestures like crossing arms or standing with a closed posture may be interpreted as ambiguous or defensive (Fig. 2(d)). The robot responds with non-engaging actions, such as placing a hand on its torso to signal caution or emotional distance.

e) Aggressive: When the user simulates an attack—e.g., making fists and adopting a boxing stance (Fig. 2(f))—the robot classifies the intent as aggressive. It reacts with protective motions such as a punch or defensive block, signaling readiness to de-escalate or maintain safety.

f) Ambiguous: In cases where the user’s posture does not clearly convey a specific intent—such as minimal arm movement or occluded gestures, the system classifies the interaction context as ambiguous. To ensure safety and maintain social appropriateness, the robot defaults to neutral or non-intrusive motions, such as cross arms.

C. Intention aware via In-Context Learning

To evaluate whether our vision-language model, prompted via in-context learning, can accurately infer human intent and generate contextually appropriate motions, we define five core categories of interaction: *Greeting*, *Supportive*, *Neutral*, *Defensive*, *ambiguous*, and *Aggressive*. Based on these interaction context inference and confidence score, to further evaluate the Intention awareness module. Although Fig. 2 presents representative examples of each category, we further conduct several experiment to evaluate the intention awareness to further push the limitation of it.

a) Standard Interaction Evaluation: To assess the intention-aware module’s ability to interpret human upper-body gestures via in-context learning, we evaluate its performance across six representative interaction categories. As shown in Table I, the model achieves high classification accuracy in structured scenarios, particularly for Greeting and Aggressive behaviors. In contrast, Ambiguous cases exhibit reduced accuracy and frequent fallback activations, reflecting appropriate uncertainty-aware behaviour. These results indicate that the system can robustly infer intent in most social contexts, while conservatively responding under uncertainty.

b) Modality Ablation: To evaluate the contribution of each input modality to human intention inference, we conduct an ablation study using ten challenging

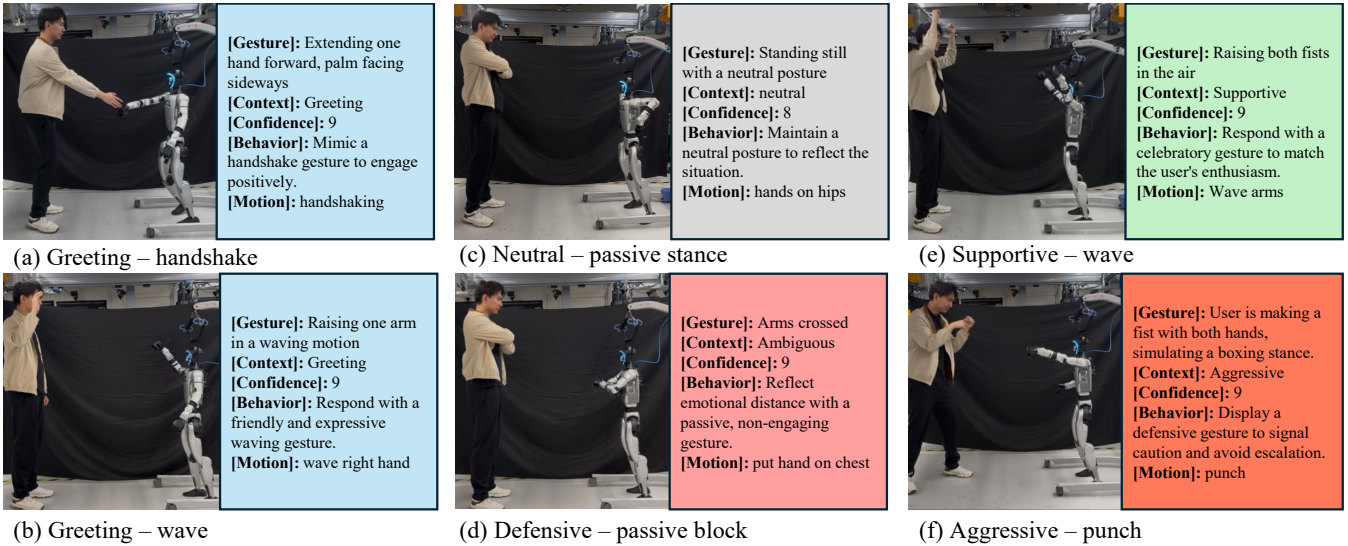


Fig. 2: Human-Robot Interaction Scenarios: Representative interaction scenarios for evaluating the vision-language intention reasoning module. Each pair shows a user gesture (left) and the robot’s inferred response (right), including confidence, context, and selected motion. Background colors denote interaction categories: blue (Greeting), green (Supportive), gray (Neutral), pink (Defensive), and orange (Aggressive).

TABLE I: Summary of Inferred Robot Behaviors Across Six Interaction Scenarios

Scenario Type	Samples	Context Accuracy	Avg Confidence	Fallback Triggered	Example Motion
Greeting	12	12 / 12 (100%)	9.3	0	wave right hand, handshaking
Supportive	8	5 / 8 (62.5%)	8.75	0	wave arms
Neutral	8	7 / 8 (87.5%)	7.27	2	hands on hips, put hand on chest
Defensive	13	12 / 13 (92.3%)	8.00	0	cross arms
Ambiguous	15	10 / 15 (66.6%)	5.40	10	shrugging, cross arms
Aggressive	15	15 / 15 (100%)	8.13	0	punch

TABLE II: Ablation study on input modality.

Input Modality	Interaction Context Accuracy
Prompt only	0.5
Image only	0.4
Combined	0.9

test cases involving ambiguous or low-confidence gestures—such as partial occlusion, subtle upper-body motion, or low-light conditions. We compare three input configurations: vision-only, language-only, and combined vision-language input. As summarised in Table II, the combined modality achieves substantially higher classification accuracy than either modality alone, underscoring the complementary strengths of visual and linguistic information for robust social context reasoning. This also supports the integration of fallback mechanisms when relying on single-modality input under uncertainty.

c) Iterative Intention Refinement: Our system supports real-time intention refinement by continuously updating its inference based on incoming observations and interaction history. When the initial gesture is ambiguous or misinterpreted, subsequent clearer actions can override the previous prediction, allowing the robot to adapt its behavior accordingly. This is enabled by the rolling

TABLE III: Executable Motions and Expressiveness on Real Robot

Motion	Generated	Expressive
wave right hand	✓	✓
cross arms	✓	✓
hands on hips	✓	✓
beat gestures	✓	✓
punch	✓	✓
handshaking	✓	✓
handover	✓	✓
think	✓	✓
shrugging / showing palms	✓	✗
throw	✓	✗
hug (spread arms)	✓	✗
clap hands	✓	✗

input mechanism and temporal awareness within the in-context prompting structure.

d) Generalization: Our designed system demonstrates preliminary generalization in multi-person scenarios, the vision-language model tends to focus on the individual exhibiting the most salient upper-body motion. This prioritization enables robust intention inference even when multiple people are present, without requiring explicit person tracking.

e) Social-awareness: In addition, we observe emergent social-context sensitivity, where the robot adapts its responses based on interaction history and perceived familiarity. For instance, in repeated interactions, the system tends to select more positive or engaging gestures for previously encountered users, while exhibiting more cautious behavior when confronted with unfamiliar or ambiguous motions.

D. Expressive Motions Execution on Real Robot

In this section, we evaluate the physical executability and expressiveness of generated upper-body gestures on the G1 humanoid robot. Our goal is to determine which motion prompts can be reliably generated by DART, retargeted, and executed in real-world conditions while preserving their intended social meaning.

Due to hardware constraints and the challenges of whole-body balancing, we focus exclusively on upper-body motions involving the arms and torso. Each gesture is evaluated for (i) whether the diffusion model can generate the motion based on a brief textual prompt, and (ii) perceived expressiveness. While all motions were physically executable, some lost semantic clarity due to limited joint range, motion smoothness, or retargeting artifacts.

We group motions into two categories: those that remain expressive on the robot (top of Table III) and those with reduced expressiveness despite successful execution (bottom). This highlights the practical gap between planned gestures and embodied expression.

Through our experiments, some limitations stem not from hardware, but from the motion generation stage itself. For instance, *clap hands* frequently exhibits self-penetration artifacts during synthesis, especially when hand trajectories intersect rapidly or without spatial clearance. Such artifacts degrade realism and compromise the motion’s suitability for retargeting or social interpretation.

E. Real Human-Robot Interaction Test

We validate the full pipeline across three aspects: latency, interaction scenarios, and failure analysis. The system operates asynchronously, with real-time modules for image capture, intention inference, and motion execution.

a) Interaction scenarios: showcase successful human-robot interactions in Fig. 2, covering common scenarios such as greetings, object handover, neutral poses, and ambiguous or defensive gestures. Each case includes the user’s upper-body behavior, inferred intention and confidence, contextual interpretation, and the robot’s executed gesture. These examples demonstrate the system’s ability to interpret subtle social cues and respond with contextually appropriate, non-verbal physical gestures.

TABLE IV: Latency of Each Module in the Real-Time Pipeline

Module	Latency (s)
Video Capture	0.7 (continuous, async)
VLM Inference	4.05 (avg), 1.72–11.83
Motion Generation	0.087 (avg per 8 frames)
Motion Execution	0 (streamed at 500 Hz)

b) System latency: is a critical factor in evaluating the responsiveness of the pipeline for real-time human-robot interaction. Although each module introduces its own delay, the system operates asynchronously, so these latencies do not accumulate linearly. The vision module continuously captures three frames every 0.7s, while the VLM inference runs in a separate thread, processing new input only after the previous cycle completes. The motion generation and execution module maintains its current action until a new prompt is received.

The primary bottleneck lies in VLM inference. We measured GPT-4o inference latency over 62 trials, with times ranging from 1.72 s to 11.83 s, averaging 4.05 s (median 3.62 s). 95% of responses completed within 7.98 s, supporting semi-real-time HRI. DART generates 8-frame motion segments at 25 FPS. Each rollout takes 0.087 s on average (range: 0.057–0.116 s) and is computed 4 frames ahead to ensure continuity. The generated motions are interpolated at 500 Hz and streamed as Euler angles to the low-level PD controller. Table IV summarizes the latency breakdown.

c) Failure Discussion: During deployment, we observed that some gestures, such as hug and clap hands, fail to convey their intended meaning on the physical robot due to joint limitations. To address this, we add motion constraints in the VLM pre-prompt, excluding unreliable gestures or replacing them with more expressive alternatives (e.g., substituting hug with spread arms).

Another source of error stems from ambiguous or degraded visual input. Low lighting, occlusions, or subtle user motion can lead to inaccurate intention inference. To mitigate this, we incorporate a confidence-aware filtering mechanism that suppresses uncertain outputs and triggers fallback gestures when appropriate.

A third challenge arises from latency variability in GPT-4o, where occasional inference delays can disrupt interaction fluidity. While most responses complete within 4 seconds, we observed spikes exceeding 10 seconds in rare cases. To mitigate this, we maintain asynchronous module execution and pre-generate motion segments in parallel, allowing the robot to continue default or ongoing actions while awaiting new prompts.

Despite the promising results achieved by integrating vision-language models for pose classification and gesture selection, we observe practical limitations when deploying such systems via commercial APIs like GPT-4o. The system may reject the query due to internal

safety constraints. These built-in moderation filters are designed to prevent misuse but can inadvertently block legitimate robot reasoning tasks. As a result, inference is occasionally disrupted or denied, limiting the robustness of real-time deployment.

V. CONCLUSION

We have presented HIAER, a hierarchical framework that combines intention-aware inference through ILC with real-time diffusion-based motion generation. By leveraging carefully designed pre-prompts and few-shot examples, our approach effectively guides a VLM to accurately identify human intentions. Additionally, integrating the DART generative model ensures smooth, real-time motion generation and seamless transitions between expressive gestures. This allows humanoid robots to deliver socially appropriate and physically executable upper-body responses during interactive scenarios.

Future work will explore full-body motion integration through whole-body control and real-time joint-space tracking, as well as extending the framework to support multi-party interaction and long-term human-robot engagement.

REFERENCES

- [1] V. Chidambaram, Y.-H. Chiang, and B. Mutlu, "Designing persuasive robots: How robots might persuade people using vocal and nonverbal cues," in *2012 7th ACM/IEEE International Conference on Human-Robot Interaction*, 2012, pp. 293–300.
- [2] C.-M. Huang and B. Mutlu, "Modeling and evaluating narrative gestures for humanlike robots," in *Robotics: Science and Systems*, vol. 2. Citeseer, 2013.
- [3] M. Salem, S. Kopp *et al.*, "Generation and evaluation of communicative robot gesture," *International Journal of Social Robotics*, vol. 4, pp. 201–217, 2012.
- [4] C. Y. Kim, C. P. Lee, and B. Mutlu, "Understanding large-language model (llm)-powered human-robot interaction," in *Proceedings of the 2024 ACM/IEEE international conference on human-robot interaction*, 2024, pp. 371–380.
- [5] S. Gupta and A. Kumar, "A brief review of dynamics and control of underactuated biped robots," *Advanced Robotics*, vol. 31, pp. 607–623, 2017.
- [6] L. Bao, J. Humphreys *et al.*, "Deep reinforcement learning for bipedal locomotion: A brief survey," *arXiv preprint arXiv:2404.17070*, 2024.
- [7] Z. Gu, J. Li *et al.*, "Humanoid locomotion and manipulation: Current progress and challenges in control, planning, and learning," 2025. [Online]. Available: <https://arxiv.org/abs/2501.02116>
- [8] G. Laban, J.-N. George *et al.*, "Tell me more! assessing interactions with social robots from speech," *Paladyn, Journal of Behavioral Robotics*, vol. 12, no. 1, pp. 136–159, 2021. [Online]. Available: <https://doi.org/10.1515/pjbr-2021-0011>
- [9] A. Aly and A. Tapus, "A model for synthesizing a combined verbal and nonverbal behavior based on personality traits in human-robot interaction," in *2013 8th ACM/IEEE International Conference on Human-Robot Interaction*, 2013, pp. 325–332.
- [10] Z. Li, C. Cummings, and K. Sreenath, "Animated cassie: A dynamic relatable robotic character," in *2020 IEEE/RSJ International Conference on Intelligent Robots and Systems*, 2020, pp. 3739–3746.
- [11] S. Min, X. Lyu *et al.*, "Rethinking the role of demonstrations: What makes in-context learning work?" in *EMNLP*, 2022.
- [12] P. Huang, Y. Hu *et al.*, "Emotion: Expressive motion sequence generation for humanoid robots with in-context learning," *arXiv preprint arXiv:2410.23234*, 2024.
- [13] K. Zhao, G. Li, and S. Tang, "DartControl: A diffusion-based autoregressive motion model for real-time text-driven motion control," in *The Thirteenth International Conference on Learning Representations*, 2025.
- [14] C. Breazeal, "Emotion and sociable humanoid robots," *International Journal of Human-Computer Studies*, vol. 59, no. 1, pp. 119–155, 2003.
- [15] X. Cheng, Y. Ji *et al.*, "Expressive whole-body control for humanoid robots," *arXiv preprint arXiv:2402.16796*, 2024.
- [16] T. He, Z. Luo *et al.*, "OmniH2o: Universal and dexterous human-to-humanoid whole-body teleoperation and learning," *arXiv preprint arXiv:2406.08858*, 2024.
- [17] D. Porfirio, E. Fisher *et al.*, "Bodystorming human-robot interactions," in *Proceedings of the 32nd Annual ACM Symposium on User Interface Software and Technology*. Association for Computing Machinery, 2019, p. 479–491. [Online]. Available: <https://doi.org/10.1145/3332165.3347957>
- [18] Y.-J. Wang, B. Zhang *et al.*, "Prompt a robot to walk with large language models," in *IEEE Conference on Decision and Control*, December 2024.
- [19] S. Sun, C. Li *et al.*, "Leveraging large language models for comprehensive locomotion control in humanoid robots design," *Biomimetic Intelligence and Robotics*, vol. 4, no. 4, p. 100187, 2024.
- [20] H. Ahn, T. Ha *et al.*, "Text2action: Generative adversarial synthesis from language to action," in *2018 IEEE International Conference on Robotics and Automation*, 2018, pp. 5915–5920.
- [21] C. Guo, X. Zuo *et al.*, "Action2motion: Conditioned generation of 3d human motions," in *Proceedings of the 28th ACM International Conference on Multimedia*, 2020, pp. 2021–2029.
- [22] J. Ho, A. Jain, and P. Abbeel, "Denoising diffusion probabilistic models," *Advances in neural information processing systems*, vol. 33, pp. 6840–6851, 2020.
- [23] G. Tevet, S. Raab *et al.*, "Human motion diffusion model," in *The Eleventh International Conference on Learning Representations*, 2023. [Online]. Available: <https://openreview.net/forum?id=SJ1kSyO2jwu>
- [24] N. Mahmood, N. Ghorbani *et al.*, "Amass: Archive of motion capture as surface shapes," in *2019 IEEE/CVF International Conference on Computer Vision*, 2019, pp. 5441–5450.
- [25] C. Guo, S. Zou *et al.*, "Generating diverse and natural 3d human motions from text," in *Proceedings of the IEEE/CVF Conference on Computer Vision and Pattern Recognition*, June 2022, pp. 5152–5161.
- [26] K. Mahadevan, J. Chien *et al.*, "Generative expressive robot behaviors using large language models," in *Proceedings of the 2024 ACM/IEEE International Conference on Human-Robot Interaction*, 2024, p. 482–491.
- [27] OpenAI, A. Hurst *et al.*, "Gpt-4o system card," 2024. [Online]. Available: <https://arxiv.org/abs/2410.21276>
- [28] Unitree Robotics, "Unitree g1 humanoid robot," <https://www.unitree.com/g1>, 2024, accessed: 2025-05-13.
- [29] Y. Zhou, C. Barnes *et al.*, "On the continuity of rotation representations in neural networks," in *Proceedings of the IEEE/CVF conference on computer vision and pattern recognition*, 2019, pp. 5745–5753.